THE ASTROPHYSICAL JOURNAL, 522:L29–L33, 1999 September 1

FIRST EXTRAGALACTIC DIRECT DETECTION OF LARGE-SCALE MOLECULAR HYDROGEN IN THE DISK OF NGC 891[1]

EDWIN A. VALENTIJN[2]
Kapteyn Institute and Space Research Organization of the Netherlands, P.O. Box 800,
NL-9700 AV Groningen, The Netherlands; valentyn@astro.rug.nl
AND
PAUL P. VAN DER WERF
Leiden Observatory, P.O. Box 9513, NL-2300 RA Leiden, The Netherlands; pvdwerf@strw.leidenuniv.nl
Received 1999 April 6; accepted 1999 July 6; published 1999 August 5

ABSTRACT

We present direct observations of molecular hydrogen in the disk of the nearby edge-on spiral galaxy NGC 891. With *Infrared Space Observatory*'s Short-Wavelength Spectrometer (SWS) it has been possible, for the first time, to observe the lowest pure rotational lines of H_2 [$S(0)$ at 28.2 μm and $S(1)$ at 17.0 μm] at eight positions throughout the stellar disk of NGC 891. Both lines have been detected at all the surveyed positions out to 11 kpc north of the center of the galaxy. An H_2 rotation curve is derived, and we compare H_2 radial profiles with CO and H I data. The observed line ratios indicate relatively warm (T = 150–230 K) molecular clouds scattered throughout the disk in addition to a massive cooler (T = 80–90 K) component which dominates the signal in the outer regions. For H_2 ortho/para ratios of 2–3, the cool gas has typical edge-on column densities (1–3) × 10^{23} cm^{-2} (or ~3000 $M_\odot$ pc^{-2}), in which case it outweighs the H I by a factor of 5–15. This factor matches well the mass required to resolve the problem of the missing matter of spiral galaxies within at least the optical disk. The newly discovered cool H_2 component would be less massive in the case in which its dominant ortho/para ratio is near unity. We address the thermal balance of this component by a comparison with [C II] 158 μm data. When combining the new coolish molecular gas results with recent SCUBA cold dust observations of NGC 891, the total gas-to-dust ratio at $r < 12$ kpc remains around 200.

Subject headings: dark matter — galaxies: individual (NGC 891) — galaxies: ISM — ISM: molecules

1. INTRODUCTION

The gaseous interstellar medium in galaxies consists essentially of atomic and molecular hydrogen. While atomic hydrogen has been extensively mapped in the 21 cm line in many galaxies and found to account for roughly 10% of their dynamic mass, their H_2 content is very uncertain, since it is estimated only indirectly.

Before the launch of the *Infrared Space Observatory* (*ISO*), H_2 emission in external galaxies was only detected in rovibrational lines near 2.1 μm, from typically 10^4 $M_\odot$ of H_2, heated to temperatures of ~2000 K in the centers of starburst, active, and (ultra)luminous infrared galaxies. At lower temperatures, these lines are too faint, and most of our knowledge about the H_2 content comes from observations of CO, assuming a CO/H_2 conversion factor derived for Galactic giant molecular clouds (e.g., Solomon et al. 1987).

ISO's Short-Wavelength Spectrometer (SWS; de Graauw et al. 1996) provides a unique possibility to observe moderately warm H_2 directly in the lowest purely rotational quadrupole transitions $S(0)$: J_u–J_l = 2–0 at 28.2188 μm and $S(1)$: J_u–J_l = 3–1 at 17.0348 μm, belonging to respectively the ortho (J-odd) and para (J-even) series. The ortho/para ratio (hereafter o/p) will be 3 if set by the ratio of statistical weights.

The first extragalactic detection of these lines in the central, relatively warm, and star-forming region of a galaxy was reported for NGC 6946, and we refer readers to Valentijn et al. (1996b) for further details of the survey. For NGC 6946, the observed line ratio [$S(0)/S(1) \sim 0.15$] indicated a temperature of this gas component of 170 K for an o/p = 3. A significant upper limit on the $S(2)$ (12.3 μm) line flux was used to constrain the o/p to $\geq$2, a value which is also commonly found for photon-dominated regions (PDRs).

Complementary to the H_2 rovibrational line surveys and most of the extragalactic *ISO* program, we have selected a relatively normal, nonstarbursting galaxy, NGC 891, and surveyed its disk. We positioned the SWS apertures at eight positions along the galaxy's major axis: out to 11 kpc north and 8 kpc south of the nucleus. We have selected this target because of the expected high column densities from an edge-on disk and because of its proximity (we assume here a distance of 9.5 Mpc).

2. OBSERVATIONS

We observed each line for ~1500 s with the SWS grating (AOT 2 observing mode) using the BIBIB Si:As detector array, which has the advantages of the near absence of hysteresis effects and a very stable (within a few percent) response. The in-flight flux calibration (Schaidt et al. 1996) of this detector matched within 10% to the preflight value measured on a blackbody of known temperature. However, in flight, the effects of impact of cosmic rays on both the detectors and the electronics were severe, and we had to develop dedicated glitch recognition and removal programs (Valentijn & Thi 1999). Thus, we could reduce the effective noise level by a factor of ~4 to ~0.1 Jy and achieve spectra in which the noise fluctuations are nearly normally distributed. One position, at 11 kpc north, was observed in total for 4 hr as a confirmation of our key results.

Figures 1 and 2 show our observational data. We have detected both lines at all the observed positions at a signal-to-

[1] Based on Observations made with *ISO*, an ESA project with instruments funded by ESA member states (especially the PI countries: France, Germany, the Netherlands, and the United Kingdom) and with the participation of ISAS and NASA.

[2] Now at Kapteyn Institute, Groningen, The Netherlands.

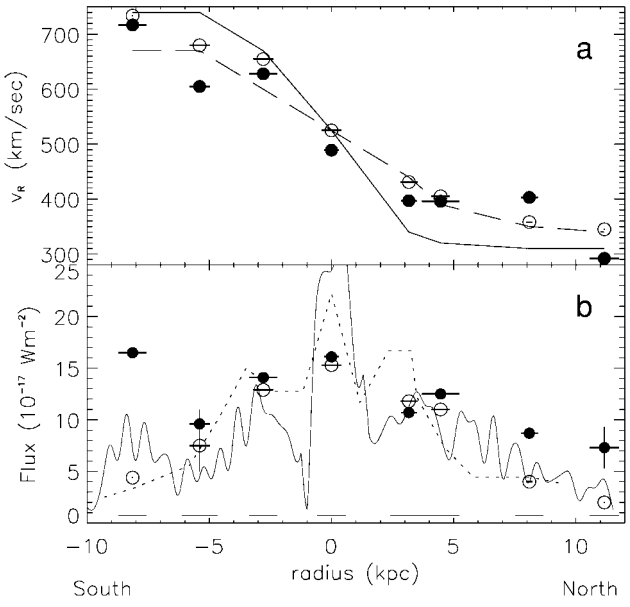

FIG. 1.—Observations of H_2 *S*(0) (*filled circles*) and *S*(1) (*open circles*) at various positions along the major axis of NGC 891. The sizes of the emitting regions, projected along the major axis, are indicated by horizontal bars through the data points. The horizontal bars at the bottom of panel *b* indicate the size of the SWS aperture [for *S*(0)] projected along the major axis. (*a*) Heliocentric radial velocities; the lines indicate the approximate maximum and minimum rotational velocities from ^{12}CO data of Sakamoto et al. (1997). (*b*) Total line strength within the SWS aperture. ^{12}CO 1–0 intensity profiles (*drawn line*, Sakamoto et al. 1997; *dashed line*, Scoville et al. 1993) are arbitrary scaled to best fit the *S*(1) data. The exceptionally large errors on the absolute flux values of two *S*(0) lines observed late in the *ISO* mission, with aged detectors, are indicated by a vertical bar.

noise ratio of at least 5. The accuracy of the wavelength calibration (Valentijn et al. 1996a) corresponds to about 20 km s^{-1}. As the SWS slit width of 20″ at *S*(0) and 14″ at *S*(1) is a factor 2–3 larger than the diffraction beam, an offset of a point source of 4″ on the slit causes a wavelength shift corresponding to 41 km s^{-1} at *S*(1) and 53 km s^{-1} at *S*(0). When allowing for such small shifts, the observed rotational velocities match the CO data well. The effect of a slit wider than the diffraction beam also produces broader line profiles for extended sources. Since this profile broadening has been accurately characterized (Valentijn et al. 1996a), we can measure approximately the angular sizes of the emitting regions *in the direction perpendicular to the slit* (the slit length is 27″). Since the major axis of NGC 891 was positioned approximately diagonally from one slit corner to the opposite one, we projected these angular sizes along the major axis. This way, the observed line broadening indicates the size of the emitting regions in the direction along the major axis. For the direction perpendicular to the major axis, we assume that the H_2 does not extend beyond the CO disk, for which several authors find a total scale height of 5″–6″ or ~270 pc (García-Burillo et al. 1992; Scoville et al. 1993). The estimates of the source extents are used to compute the surface brightness of the lines. The source extents play a critical role in our interpretation; error bars on the extents are listed in Table 1and have been estimated using a numerical simulation of data with Gaussian line profiles with comparable signal-to-noise ratios and applying similar line extraction code. For the three outer positions, at 8 kpc north and south and 11 kpc north of the center, the *S*(1) lines are unresolved ($R = \Delta\lambda/\lambda = 2060$, 2300–2600, 2334), a highly

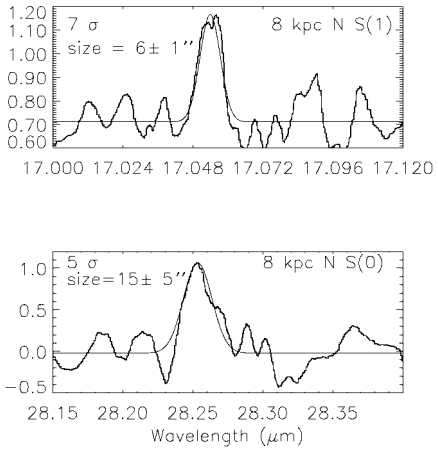

FIG. 2*a*

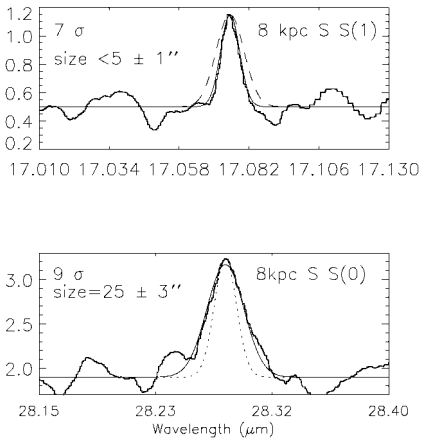

FIG. 2*b*

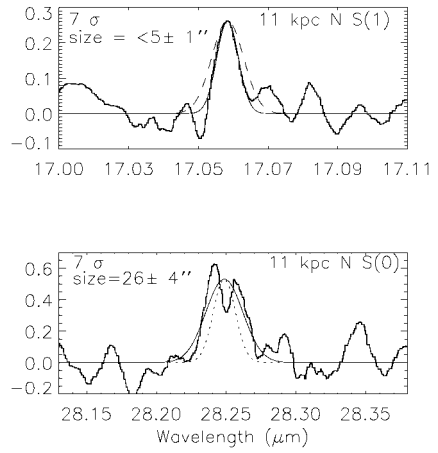

FIG. 2*c*

FIG. 2.—Observed *S*(0) and *S*(1) line profiles (total flux density in janskys within the SWS aperture) at three outer positions in NGC 891, together with Gaussian fits to the profiles (*solid lines*). The dotted lines represent the theoretical line profiles for a source extent ≤5″ perpendicular to the slit axis [identical to fits for all *S*(1) lines] and correspond to a spectral resolution of 200 and 134 km s^{-1} for respectively *S*(0) and *S*(1). The long dashed lines represent the theoretical profiles for a source extent filling the slit [identical to the best fit for *S*(0) at 8 kpc south and 11 kpc north]. The best fit for *S*(0) 8 kpc north corresponds to a source extent of 15″ projected along the galaxy major axis.

TABLE 1

MOLECULAR HYDROGEN IN THE DISK OF NGC 891

Radius (kpc)	T (K)	n_{H_2} (cm^{-3})	N_{H_2} (10^{22} cm^{-2})	σ H_2 (10^2 $M_\odot$ pc^{-2})	M_{H_2} (10^7 $M_\odot$)	H_2/H I[a]	Size[b] (arcsec)
Warm Component (o/p = 3)							
−8.1	200–230	67–33	0.7–2.4	1.1–4.0	0.7–2.6	<0.3	<5 ± 1
−5.4	130–150	900–340	1.4	2.3	5.3	0.6	18
−2.8	170–200	340–200	1	1.7	5.6	0.8	25
0.0	130–170	1300–200	4–3	6–5	7–6	1.4–1.1	17
3.2	150–170	680–340	1.4	2.3	4.4	0.4	15
4.5	130–200	2000–200	1–0.6	2–1	3–2	0.3–0.2	16
8.1	170–230	200–33	1–4	2–6	1–2	<0.2	6 ± 1
11.2	230	33	2.4	3.9	1.4	<0.3	<5 ± 1
Cold Component (o/p = 2)							
−8.1	<90	200–340	≥15–11	≥25–18	≥79–56	≥9–6	25 ± 3
8.1	<90	340–680	≥10–6	≥16–10	≥30–20	≥3–2	15 ± 5
11.2	<80	68–200	≥34–13	≥55–22	≥180–72	≥31–12	26 ± 4

[a] H I within SWS aperture by R. Swaters (1999, private communication)

[b] The size for the warm component is from $S(1)$ and for the cold component from $S(0)$.

significant result. As an extra check, we have reduced with a similar code SWS observations of unresolved lines from the compact planetary nebula IC 2501 and found $R = 2300$, and intrinsically narrow $S(1)$ lines from the very extended PDR S140 and found $R = 1300$, precisely in agreement with the line profile characterization of the SWS.

3. ANALYSIS

When inspecting the radial variations in Figure 1, we note that (1) the $S(1)$ flux approximately follows the ^{12}CO 1–0 emission and drops much faster with radius than $S(0)$, so that the $S(0)/S(1)$ line ratio increases with radius and (2) the sizes of the emitting regions in $S(0)$ stay approximately constant with radius and correspond to an almost aperture filling signal, while at the three outer positions ($r = -8$, 8, and 11 kpc) the $S(1)$ line appears to originate from sources with angular sizes less than ~5″.

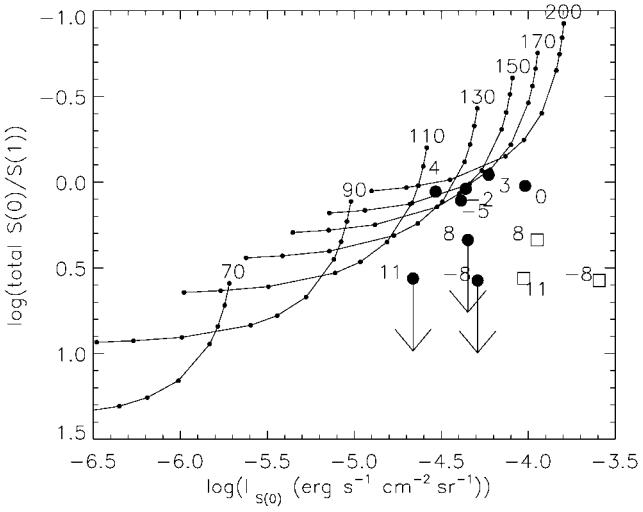

FIG. 3.—Total line intensity ratio of $S(0)$ and $S(1)$ vs. the surface brightness of the $S(0)$ line. The lines represent model data of an o/p = 3 H_2 layer with a column density $N_{H_2} = 1.4 \times 10^{22}$ cm^{-2} for various temperatures (labeled at the top of each line) and increasing density n_{H_2} (small data points on the lines correspond from left to right to values of n_{H_2} = 20, 34, 68, 200, 340, 680, 2000, 3400, 6800, and 20,000 cm^{-3}). The thick dots represent observational data using observed spatial dimensions, while the squares represent the same data for the case in which the $S(0)$ lines originate from a spatially unresolved source within each aperture, like $S(1)$.

Our H_2 survey is biased toward the warm gas, cooler gas having lower fluxes per unit mass. Therefore, in our interpretation we will focus on lower limits of H_2 mass. Below, we will detail the following interpretation: the radial variations of line strength, line ratios, and angular size indicate a relatively warm component ($T = 130$–200 K), which becomes less important at increasing radii; the $S(0)$ line originates from a cooler component ($T = 80$–90 K), which is spatially more extended (larger scale length) than $S(1)$ and dominates at large radii; thus $S(1)$ traces unresolved warm regions scattered throughout the disk, but more common in the inner regions, while $S(0)$ traces a cooler and more extended component.

We determine the component parameters by comparing the observed surface brightness with results of H_2 excitation computations. Since we have no a priori knowledge about the origin of the H_2 emission, we do our excitation computations for a single uniform layer (slab) of various H_2 temperatures, densities, and ortho-para ratios of 1, 2, and 3. These computations result in surface brightnesses which scale directly with H_2 column density (N_{H_2}). For the model data displayed in Figure 3, we chose $N_{H_2} = 1.4 \times 10^{22}$ cm^{-2}, which corresponds to the canonical value of virialized clouds, independent of their size or mass (Solomon et al. 1987), but we did not explicitly assume the virial condition to apply. The lines in Figure 3 thus represent the expected H_2 properties of single molecular clouds of a given temperature, with N_{H_2} such as typically encountered in the Milky Way, but can equally well be taken as the properties of H_2 layers with given parameter values. If more than one, or alternatively, higher N_{H_2}, clouds/layers are located along the line of sight, the observed data points should be located to the right of the lines of the model clouds. Thus we can use Figure 3 to match the observations to a range of "model cloud" parameter values.

In Table 1 we list our results, preferring the highest T (lowest H_2 density) solutions, which lead to the lowest inferred H_2 masses. For each position we list the allowed range of temperatures, N_{H_2} and the corresponding H_2 edge-on mass densities, and total H_2 mass within the aperture. For the positions at radii smaller than 6 kpc, we find that the observed lines can be well matched with clouds with temperatures in the range 130–230 K, $n_{H_2} \sim 200$–2000 cm^{-3} and $N_{H_2} \sim 10^{22}$ cm^{-2}, with a factor of 3 times higher N_{H_2} in the center of NGC 891. Since all the

spectral lines are broadened at most of the $r < 6$ kpc positions, these values correspond to, on average, about one "model cloud" along the line of sight *everywhere* within the part of the disk covered by the aperture, implying a total of (3–5) $\times$ 10^7 $M_\odot$ of warm H_2 per observed position. Interpolating over the whole region $r < 6$ kpc, this corresponds to $\sim 2 \times 10^9 M_\odot$ of warm H_2, roughly half of the mass deduced from CO data (Sofue & Nakai 1993; Sakamoto et al. 1997) in the same region. Given its temperature and density, this large amount of warm gas can be identified with the UV-heated outer layers of molecular clouds throughout the inner disk of NGC 891, where CO may be photodissociated. This interpretation is in agreement with the detection of extended [C II] 158 μm emission in NGC 891 (Madden et al. 1994), originating in warm extended PDRs. These warm PDRs thus contain a significant fraction of the gas mass in the inner disk of NGC 891.

For our analysis of the three outer positions at $r = -8$, 8, and 11 kpc, we first assume the "warm component" also to dominate both $S(1)$ and $S(0)$. As $S(1)$ is definitely unresolved ($<5''$), and insisting here on a one-component solution, the size of $S(0)$ must also be less than $5''$. These angular sizes then propagate into surface brightness values as indicated by the three squares at the right-hand side of Figure 3. These points indicate clouds of extremely high column density, or tens of "model clouds" per position. However, this is a problem because it appears impossible to have, by chance, so many clouds concentrated in $5''$ regions in each of these three $14''$ apertures. Thus the simple fact that the $S(1)$ lines are unresolved, implying unresolved $S(0)$ in one-component models, prompts us to consider a two-component model with one component related to unresolved $S(1)$ and the other component related to resolved, essentially slit filling, $S(0)$. In fact, this interpretation is supported by the actually observed $S(0)$ line width. More quantitatively, if at least two-thirds of the $S(1)$ emission originates in the warm component, consisting of one or a few warm clouds per aperture, the problem encountered above in the one-component model disappears. For the computation of $I_{S(0)}$ of the cooler component, we now have to use the observed large $S(0)$ sizes: thus we obtain the data points near the tips of the arrows in Figure 3. The cooler component as indicated by $S(0)$ should then arise from dozens to hundreds of clouds along the line of sight with a total edge-on column density in the range (1–3) $\times$ 10^{23} cm^{-2} (i.e., 1600–5500 $M_\odot$ pc^{-2}) and temperatures in the range 80–90 K. For these computations we used o/p = 2 (see below). The total mass of this extended H_2 is in the range (0.3–1.8) $\times$ 10^9 $M_\odot$ *per SWS aperture.* In Figure 1*b* this extended cooler component is seen as an excess of $S(0)$ emission at all the three outer positions, when compared to $S(1)$ and CO radial profiles. In the case of the position at 8 kpc south, the extreme $S(0)$ flux coincides with a region with an enhanced CO signal.

4. DISCUSSION

The presence of a large amount of fairly warm molecular gas raises the issue of its thermal balance. Elevated temperatures may result from efficient heating, inefficient cooling, or both. While heating by stellar radiation is normally the principal heating mechanism, additional heat input may be provided by cosmic rays, which is expected to be an order of magnitude more important in NGC 891 than in the Milky Way, as shown by its much more intense synchrotron radiation. Cooling of moderate density, warm molecular gas is normally dominated by [C II] 158 μm emission. However, *ISO* spectroscopy has revealed a strong deficiency of [C II] cooling under a wide variety of circumstances (Malhotra et al. 1997; Fisher et al. 1998; Luhman et al. 1998). Such a deficiency would in the present case naturally lead to the observed warm gas component, and actually H_2 might become the dominant cooler. This hypothesis can be tested directly using existing [C II] 158 μm measurements of NGC 891 (Madden et al. 1994). The expected cooling by [C II] 158 μm emission from the massive H_2 component is (1–2) $\times$ 10^{-3} ergs s^{-1} cm^{-2} sr^{-1} if all carbon (assumed to have solar abundance) is in the form of C^+. The measured value is a factor of 5–10 lower (Madden et al. 1994). The origin of this suppression of [C II] cooling may be ascribed to a lower C^+ abundance, optically thick [C II] emission, self-absorption in the 158 μm line, or other mechanisms; this issue is currently the subject of considerable debate, and hence more detailed analysis is beyond the scope of the present Letter. Regardless of its origin, however, suppression of the principal cooling mechanism is a natural way of producing elevated temperatures.

For the H_2 mass determination, it is essential that we estimate the o/p correctly. Low values (o/p $\ll 2$, resulting in $\sim$4 times lower masses) are found only in the very cold gas sampled by absorption measurements (Lacy et al. 1994). The elevated temperatures derived here show that different conditions prevail in the gas detected here and point toward PDRs in the warm, moderate-density envelopes of molecular clouds. Direct measurements in such regions consistently indicate o/p $\sim$ 2 (Hoban et al. 1991; Chrysostomou et al. 1993; Ramsay et al. 1993; Valentijn et al. 1996b; Harrison et al. 1998). However, recently Sternberg & Neufeld (1998) pointed out that these observed values might still imply an intrinsic o/p = 3. While o/p = 3 would result in higher masses by a factor of 2, we thus take the more conservative approach of an o/p = 2 for deriving our strict lower limits.

Our analysis indicates a 80–90 K H_2 component which outweighs the H I by a factor of 5–15. Such a massive component, for which we find a radial scale length (>12 kpc) of $S(0)$ larger than that of the stars (as is also the case for H I), matches to earlier suggestions about the possibility of a baryonic massive component resident in the disks of spiral galaxies, which dominates the potential and the rotation curves (e.g., Valentijn 1991; González-Serrano & Valentijn 1991; Lequeux, Allen, & Guilloteau 1993; Pfenniger, Combes, & Martinet 1994; Gerhard & Silk 1996), at least in the regions observed here, i.e., in the outer stellar disk. The result is also in line with opacity studies (Valentijn 1990), which suggested relatively high column densities of H_2, even at larger radii, possibly associated with a dust component with a face-on optical depth around unity and a scale length larger than that of the stars. Recent ISOPHOT observations reveal massive cool dust components (Krügel et al. 1998) with a scale length larger than that of the stars (Alton et al. 1998b), which has also been reported in the outer regions of NGC 891 from the analysis of SCUBA submillimeter images (Alton et al. 1998a). Within $r = 11$ kpc, 5 $\times$ 10^7 $M_\odot$ of cold ($T \sim 15$ K) dust is found, i.e., 8.6 $M_\odot$ pc^{-2}, while H I studies (Swaters, Sancisi, & van der Hulst 1998) mapped 75 $M_\odot$ pc^{-2}. Thus, these results can be used to estimate an overall gas-to-dust ratio in the disk of NGC 891 at $r < 11$ kpc: $[N(H_2) + N(\text{H I})]/\text{dust} = (1600 + 75)/8.6 = 200$, which is near the Galactic value.

Although our results provide support for the presence of baryonic dark matter in the disks of spiral galaxies (in the form of H_2), they also call for further studies on the physics of the interstellar medium, particularly regarding the heating mechanism, the [C II] emission deficiency, ortho/para ratios, and gas-to-dust ratios.

We thank the SIDT at VILSPA and D. Boxhoorn for their support, S. Sakamoto and R. Swaters for providing us respectively with CO and H I data, and A. G. G. M. Tielens for stimulating comments. Additional observing time for the SWS H_2 survey has been granted by Th. de Graauw and M. F. Kessler.

REFERENCES

Alton, P. B., Bianchi, S., Rand, R. J., Xilouris, E. M., Davies, J. I., & Trewhella, M. 1998a, ApJ, 507, L125
Alton, P. B., et al. 1998b, A&A, 335, 807
Chrysostomou, A., Brand, P., Burton, M., & Moorhouse, A. 1993, MNRAS, 265, 329
de Graauw, Th., et al. 1996, A&A, 315, L49
Fischer, J., et al. 1998, in Extragalactic Astronomy in the Infrared, ed. G. A. Mamon, T. X. Thuan, & J. T. T. Van (Gif-sur-Yvette: Editions Frontières), 289
García-Burillo, S., Guélin, M., Cernicharo, J., & Dahlem, M. 1992, A&A, 266, 21
Gerhard, O., & Silk, J. 1996, ApJ, 472, 34
González-Serrano, I., & Valentijn, E. A. 1991, A&A, 242, 334
Harrison, A., Puxley, P., Russel, A., & Brand, P. 1998, MNRAS, 297, 624
Hoban, S., Reuter, D. C., Mumma, M. J., & Storrs, A. D. 1991, ApJ, 370, 228
Krügel, E., Siebenmoren, R., Zota, V., & Chini, R. 1998, A&A, 331, L9
Lacy, J. H., Knacke, R., Geball, T. R., & Tokunaga, A. T. 1994, ApJ, 428, L69
Lequeux, J., Allen, R. J., & Guilloteau, S. 1993, A&A, 280, L23
Luhman, M. L., et al. 1998, ApJ, 504, L11
Madden, S. C., Geis, N., Genzel, R., Herrmann, F., Poglitsch, A., Stacey, G. J., & Townes, C. H. 1994, Infrared Phys. Technol., 35, 311
Malhotra, S., et al. 1997, ApJ, 491, L27
Pfenniger, D., Combes, F., & Martinet, L. 1994, A&A, 285, 79
Ramsay, S. K., Chrysostomou, A., Geballe, T. R., Brand, P. W. J. L., & Mountain, M. 1993, MNRAS, 263, 695
Sakamoto, S., Handa, T., Sofue, Y., Honma, M., & Sorai, K. 1997, ApJ, 475, 134
Schaidt, S. S., et al. 1996, A&A, 315, L55
Scoville, N. Z., Thakkar, D., Carlstrom, J. E., & Sargent, A. I. 1993, ApJ, 404, L59
Sofue, Y., & Nakai, N. 1993, PASJ, 45, 139
Solomon, P. M., Rivolo, A. R., Barrett, J. W., & Yahil, A. 1987, ApJ, 319, 730
Sternberg, A., & Neufeld, A. 1998, preprint (astro-ph/9812049)
Swaters, R. A., Sancisi, R., & van der Hulst, J. M. 1998, ApJ, 491, L140
Valentijn, E. A. 1990, Nature, 346, 153
———. 1991, in IAU Symp. 144, The Interstellar Disk–Halo Connection in Galaxies, ed. H. Bloemen (Dordrecht: Kluwer), 245
Valentijn, E. A., et al. 1996a, A&A, 315, L60
Valentijn, E. A., & Thi, W. F. 1999, Exp. Astron., in press
Valentijn, E. A., van der Werf, P. P., de Graauw, Th., & de Jong, T. 1996b, A&A, 315, L145